RESEARCH ARTICLE

Particles and iodine compounds in coastal Antarctica

Howard K. Roscoe[1], Anna E. Jones[1], Neil Brough[1], Rolf Weller[2], Alfonso Saiz-Lopez[3], Anoop S. Mahajan[4], Anja Schoenhardt[5], John P. Burrows[5], and Zoe L. Fleming[6]

[1]British Antarctic Survey, Cambridge, UK, [2]Alfred Wegener Institute, Bremerhaven, Germany, [3]Atmospheric Chemistry and Climate Group, Institute of Physical Chemistry Rocasolano, CSIC, Madrid, Spain, [4]Indian Institute of Tropical Meteorology, Pune, India, [5]IUP, University of Bremen, Bremen, Germany, [6]NCAS, University of Leicester, Leicester, UK

Abstract Aerosol particle number concentrations have been measured at Halley and Neumayer on the Antarctic coast, since 2004 and 1984, respectively. Sulphur compounds known to be implicated in particle formation and growth were independently measured: sulphate ions and methane sulphonic acid in filtered aerosol samples and gas phase dimethyl sulphide for limited periods. Iodine oxide, IO, was determined by a satellite sensor from 2003 to 2009 and by different ground-based sensors at Halley in 2004 and 2007. Previous model results and midlatitude observations show that iodine compounds consistent with the large values of IO observed may be responsible for an increase in number concentrations of small particles. Coastal Antarctica is useful for investigating correlations between particles, sulphur, and iodine compounds, because of their large annual cycles and the source of iodine compounds in sea ice. After smoothing all the measured data by several days, the shapes of the annual cycles in particle concentration at Halley and Neumayer are approximated by linear combinations of the shapes of sulphur compounds and IO but not by sulphur compounds alone. However, there is no short-term correlation between IO and particle concentration. The apparent correlation by eye after smoothing but not in the short term suggests that iodine compounds and particles are sourced some distance offshore. This suggests that new particles formed from iodine compounds are viable, i.e., they can last long enough to grow to the larger particles that contribute to cloud condensation nuclei, rather than being simply collected by existing particles. If so, there is significant potential for climate feedback near the sea ice zone via the aerosol indirect effect.

1. Introduction

Iodine compounds are now accepted as a source of new tropospheric particles [*O'Dowd et al.*, 2002; *Mahajan et al.*, 2010]; iodine compounds are found in large concentrations in and above the sea ice of the Weddell Sea in Antarctica in spring and summer [*Atkinson et al.*, 2012; *Schönhardt et al.*, 2008]; and new particles have been observed above the sea ice of the Weddell Sea in spring and summer [*Davison et al.*, 1996; *Atkinson et al.*, 2012]. Hence, frequent episodes of particle production in the Weddell Sea in spring and summer are expected. If this occurs near coastal stations where particle numbers are routinely measured, we might expect bursts of particles in the data.

However, in order to observe more continuous enhancement in particles, or to observe particles at coastal stations from production well offshore, new particles must become viable, i.e., grow to many tens of nanometer. In the remote marine environment, particle growth is thought to require sulphur compounds [*Charlson et al.*, 1987; *Cosme et al.*, 2005] in the form of sulphuric acid or methane sulphonic acid (MSA) from the oxidation of biogenic dimethyl sulphide (DMS), or of other condensable vapors [*Saiz-Lopez et al.*, 2012]. Uptake of sulphuric acid has been shown to enhance the formation and growth of particles from iodine oxides in laboratory experiments [*Saunders et al.*, 2010].

Figure 1, adapted from *Weller et al.* [2011], shows the annual cycle of particles at Neumayer on the Weddell Sea coast in Antarctica. By eye, there is clearly some degree of correlation of the summer maxima in sulphate and MSA with features of the annual cycle in particles. But the particle maximum occurs in autumn, and there is a secondary maximum in spring with no correlation with sulphur compounds, features which have so far been unexplained.

In this paper, we show that this secondary maximum in particles in spring arises in many years at two separate Antarctic stations and appears to be correlated by eye with observed iodine oxide (IO) near
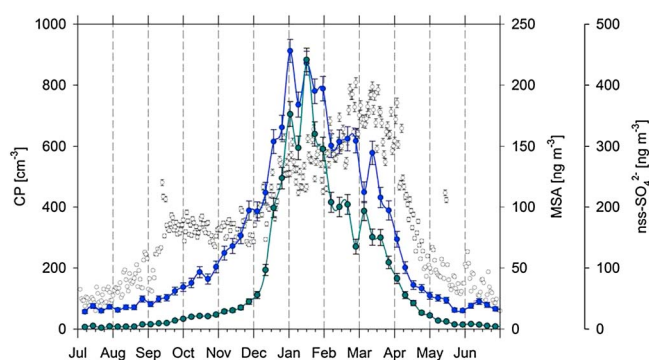
Figure 1. Mean annual cycles at Neumayer from 1991 to 2009, of concentrations of condensation particles (CP, open circles) based on daily mean values, with error bars referring to the uncertainty of the daily means; methane sulphonic acid in aerosol (MSA, green line) and nonsea-salt sulphate ion in aerosol (nss-SO_4^{2-}, blue line) both based on samples with one sigma error bars of their analytical uncertainty (adapted from data presented by *Weller et al.* [2011]). Austral spring is September/October, austral autumn is March/April. Variability can be seen from the distribution of points or changes from week to week in the lines.

those stations. The correlation occurs in time-averaged data but not in the short term, and we speculate that iodine compounds might give rise to particles which are sufficiently viable for the time-averaged correlation to occur. Coastal Antarctica is especially useful for investigating correlations between particles, sulphur, and iodine species, because of the very large annual cycles in particles and sulphur compounds, and because the Antarctic sea ice zone is a large source of iodine to the atmosphere.

2. Measurements, Methods, and Models

2.1. Measurements at Halley

Halley is located on an ice shelf 20 km from the coast of the Weddell Sea at 75.6°S, 26.8°W (Figure 2). A variety of measurements were made from the Clean Air Sector Laboratory (CASLab) located about 1 km south-east of the station, between 2004 and 2012.

2.1.1. Total Particles

Total particles exceeding 10 nm diameter were measured by a Condensation Particle Counter (TSI CPC-3010). It is operated from CASLab's central aerosol stack via an isokinetic sample line pumped at 1 l/min (see *Jones et al.* [2008] for details).

The CPC ran for three measurement periods. It operated normally from January 2004 to November 2006. From December 2006 to January 2008 and from January 2012 to November 2012, it also operated but with a reduced sensitivity (possibly due to dirt or condensation on the optics). Except for periods just after being switched back on (December 2006 and January 2012), the ratio of monthly averages in the first period to those in the second and third periods is fairly consistent with time (see Figure S1 in the supporting information), just exceeding a constant value by some 1 sigma error bars but well within 2 sigma. The ratio has a mean value of 4.35 ± 0.27. Accordingly, for all further work below, we multiply all values measured during the period of reduced sensitivity by 4.35, except for December 2006 and January 2012 which are discarded.
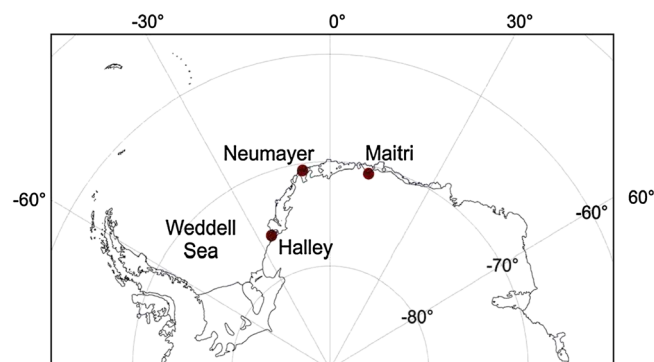

Figure 2. Map of Antarctica showing locations discussed in the text. Measurement sites are dark red circles.

The raw particle counts were averaged over 15 s intervals, which were then averaged to 1 min means (except after April 2012, when the raw averages became 1 min). To reduce file size, these 1 min values were further averaged to 10 min means for all subsequent analyses.

Because some apparent particle bursts seemed correlated with periods when the wind was from the narrow sector toward the main base, we investigated possible removal of data according to wind direction. This removed many bursts exceeding 5000/cm³. But it also removed smaller bursts, and as data removal was extended to ever wider

angles, it removed ever smaller bursts, so we were uncertain when we had reached a satisfactory range of wind directions that did not remove valid data.

Hence, we also investigated taking medians as a method of removing contaminated data. We found that daily medians gave a very similar result to a daily average after modest removal by wind direction (Figure S2 in the supporting information), so all subsequent analyses used daily medians of 10 min averages, except the analysis of short-term correlations in section 5 and Figure 9, which used hourly medians.

2.1.2. Filtered Aerosol

Filtered aerosol was collected via three different filter systems, simultaneously but with differing sampling periods and intervals: (1) lo-vol filters of 1 μm pore size, 37 mm diameter Zefluor filters (Pall-Gelman Corp.), at a flow rate of 20 L/min, sampled from CASLab's central aerosol inlet via an isokinetic sample line, for periods of 1 to 15 days; (2) hi-vol filters of Whatman 541 cellulose fiber, 254×203 mm, at a flow rate of 1000 L/min, sampled from a dedicated inlet line, from above the CASLab roof and with a shield to prevent snow ingress, for periods of 3 to 15 days; and (3) a Graseby Anderson model 236 cascade impactor was mounted on the CASLab roof with its own input system, with a shield to prevent snow ingress, where it collected the aerosol in seven-size fractions on Whatman 541 cellulose fiber filters (see *Rankin and Wolff* [2003] for more details), for periods of 10 to 20 days. Here we sum the concentrations in all size fractions.

For each system, the volume of air being sampled was measured and logged. Filters were shipped to Cambridge at −20°C and stored in Cambridge at −22°C, where they were later rinsed with ultrapure water (18 MOhm MilliQ), then analyzed for ionic content following the procedure given by *Rankin and Wolff* [2003], using a Dionex DX500 ion chromatograph (see *Obbard et al.* [2009] for chromatograph details). Here we discuss measurements of sulphate and MSA in the aerosol from December 2003 to February 2005.

2.1.3. DMS

DMS mixing ratios were measured in 2004/5, see Text S2 in the supporting information.

2.1.4. IO

IO was observed at 2 to 4 m above the surface snow by a long-path DOAS [*Saiz-Lopez et al.,* 2007] from February 2004 to February 2005. Spectra were analyzed by the DOAS technique between wavelengths of 425 and 448 nm. The resulting horizontal column densities were converted to a mean mixing ratio in the 8 km path from the lamp to the spectrometer via the distant retroreflector. Here we use the mixing ratios from the individual spectral scans, from which the plotted points and averages in *Saiz-Lopez et al.* [2007] were made, and whose mean error from the spectroscopic fit was 1.6 parts per thousand by volume (pptv). Here we use only daytime results of solar zenith angle (SZA) <85° for consistency with satellite values and take 1 day averages and averages of clusters of consecutive days (3 to 8 days). The mean standard deviation of the 1 day averages was 1.5 pptv, so most of the scatter in the individual points was due to instrument noise rather than to variability in IO. Hence, any correlation of particle bursts with increased IO in individual points, as opposed to daily averages, must be treated with caution unless the change in IO significantly exceeds 1.6 pptv.

Because in the Antarctic boundary layer the lifetime of the sum of reactive iodine gases (Iy) is short and depends on recycling via the snowpack or aerosol, we can assume that the majority of the IO is below about 40 m even if the boundary layer is thicker [*Saiz-Lopez et al.,* 2008]. Hence, we can convert the mixing ratio to an equivalent vertical amount of IO in a layer of thickness 40 m, for comparison with vertical amounts measured from satellites.

2.1.5. IO Throughout the Troposphere

IO was observed in the lower troposphere during 2007 and early 2008 by a multiaxis differential optical absorption spectroscopy (MAX-DOAS), but values were close to the detection limit (see supporting information Text S1).

2.2. Measurements at Neumayer

Neumayer is located close to the coast of the Weddell Sea near 70.7°S, 8.3°W (Figure 2). There have been three stations at Neumayer since 1981, changing location in 1992 and again in 2009. Here we discuss measurements between 1984 and 2011, made from the Air Chemistry Observatory in clean air 1.5 km south of the stations.

2.2.1. Total Particles

Total particles were measured by a series of Condensation Particle Counters. For a fuller description, see *Weller et al.* [2011], but briefly these were the following: (a) TSI CPC-3020, exceeding 10 nm diameter, from 1984 until the end of 1989; (b) TSI CPC-3760, exceeding 7 nm diameter, from 1990 until the end of 1994; (c) TSI CPC-3022(A), exceeding 7 nm diameter, from 1995 until the end of 2008; and (d) TSI CPC-3025A, exceeding 3 nm diameter, for various periods between 1996 and the present.

For measurements before 1995, concentrations were only available in daily averages. Since 1995, they were archived at hourly intervals. Below we only use values since 1995. But in order to establish the ratio of 10 nm to 7 nm size cutoff (for comparison with Halley data), we necessarily use the data from 1984 to 1989. Within error bars, the ratio is fairly consistent around the year (see Figure S3 in the supporting information): it just exceeds a constant value by some 1 sigma error bars but is well within 2 sigma and has a mean value of 1.77 ± 0.10.

2.2.2. Filtered Aerosol

Filtered aerosol was collected via high-volume sampler since 1983 with time resolution 7 to 14 days and most days since October 2003 with a two-stage system. See *Weller et al.* [2011] for details of the sampling and of the analysis to determine amounts of sulphate and MSA, as well as other ions.

2.2.3. DMS

DMS was measured in 1992/3, see Text S2 in the supporting information.

2.3. Satellite Measurements

The SCanning Imaging Absorption spectroMeter for Atmospheric CHartographY (SCIAMACHY) on European Space Agency's (ESA) Environmental Satellite (Envisat) was launched in March 2002 into an orbit with a local equator crossing time of 10 A.M. in descending node. SCIAMACHY is a combined prism and grating spectrometer that measures scattered sunlight in a wide spectral range from the UV to the near IR and in different viewing geometries. ESA lost contact with Envisat on 9 April 2012; here we discuss measurements from 2004 to 2009.

Slant columns of IO are deduced from nadir observations, by DOAS analysis from 416 to 430 nm [*Schönhardt et al.,* 2008]. The observed pixels on the ground are usually 30 km by 60 km, typically averaged to 60 km by 120 km prior to IO determination, and the instruments scans ±32° to observe a swath of width 960 km. If the albedo is large, then the sunlight scattered back to the instrument is large; hence, near the Antarctic stations we choose pixels exclusively over the ice shelves to the south and east of the stations. Noise on individual pixels is still large, so here we also average the IO data over those pixels that lie within a circle of radius 200 km centered at a point 200 km inland of each station, without cloud screening. We choose only pixels with SZA <85° to avoid possible spectral contamination by stratospheric gases and to ensure approximate consistency of air mass factors so that slant columns can be averaged. The sum of natural variability and noise on this daily data is still large enough to give significant scatter from day to day, for example, running means have standard deviations of 50 to 100%. Below, we smooth the daily data with a 10 day triangular function, which reduces the temporal noise to the useful level of 10 to 20%, as shown in the examples in several of our figures.

If the albedo is large and well defined (i.e., above a snow surface), then the Air Mass Factor (AMF, the ratio of slant to vertical path lengths) is calculated with negligible ambiguity arising from the profile shape, so the IO measurements near Antarctic stations can be translated to vertical columns. This allows them to be validated by comparison with vertical columns measured by MAX-DOAS, and with mixing ratios measured by long-path DOAS if we use the assumptions discussed in section 2.1.3. For the AMF calculation, we assume an albedo of 0.9 and no aerosol. Validation is shown in Figure S4 in the supporting information, where the SCIAMACHY values are within a factor 2 of the rescaled averaged long-path DOAS values, and reasonably follow the time dependency. This rescaling assumes that little of the IO is above the boundary layer; if in Antarctica a similar amount occurred in the free troposphere to the boundary layer (as observed in the tropical Pacific by *Dix et al.* [2013]), the differences would still be within a factor 2.

The attempt at validation using Halley MAX-DOAS data is inconclusive (Figure S5 in the supporting information), presumably due to the closeness of the observed values to the detection limit, although Figure S5 shows that the MAX-DOAS and SCIAMACHY data are indeed consistent.

2.4. The Model

Briefly, the Tropospheric Halogen Chemistry Model (THAMO) [*Saiz-Lopez et al.,* 2008] is a one-dimensional chemical transport model that includes the following characteristics:

1. The vertical resolution is 1 m. Vertical transport is from a diffusion coefficient except at the surface where it follows Monin-Obukhov similarity theory. The model domain follows an air mass trajectory.
2. The lowest level is the snowpack surface, where gas phase deposition and upward flux can occur; entrainment is via a flux of O_3 into the top level; snowpack recycling is simulated by emission fluxes of I_2 and Br_2 with Gaussian diurnal variation. The magnitude of the iodine flux is specified in the model to reproduce the observed IO.
3. The time step is 2 min, and it has state-of-the-art halogen gas phase chemistry, including self-reaction of IO to higher oxides. Usually, nonhalogens are constrained to fixed values, and temperature and relative humidity are constrained to measured values. Organic chemistry is defined by the Master Chemical Mechanism [*Saunders et al.,* 2003; *Bloss et al.,* 2005]
4. Heterogeneous chemistry is approximated in aerosol to first-order uptake; higher oxides of iodine are lost by dry deposition to the snowpack and by uptake onto preexisting aerosol.
5. Photolysis rates are calculated as a function of SZA after attenuation through fifty 1 km atmospheric layers. Albedo is specified as 0.85.
6. Dry deposition occurs for many trace gases, with deposition velocities depending on the gas.
7. Deposition to a specified aerosol surface area occurs with uptake coefficients from *Sander et al.* [2006].
8. The particle formation and growth module use higher iodine oxides (OIO, I_2O_2, I_2O_3, and I_2O_4) as the condensable species which grow through coagulation [*Saunders et al.,* 2010]. Water vapor and sulphuric acid are considered to condense leading to further growth [*Mahajan et al.,* 2010], with sulphuric acid set at 0.04 pptv in summer. The surface area of background aerosol is specified as $1e^{-7} cm^2 cm^{-3}$.

2.5. Trajectories

The UK Met Office's Numerical Atmospheric-dispersion Modelling Environment (NAME) dispersion model was used to provide footprints of where air arriving at Halley had been in the previous days. The dispersion model [*Jones et al.,* 2007] releases thousands of inert parcels of air from the site of interest and records their pathways backward in time to build a probability map of the areas that the air passed over. In our implementation, 10,000 parcels/h were released over each 3 h period for 24 h; the footprints were only recorded when air was in the lowest 100 m. The model was run backward for 1 day, 2 days, 3 days, 4 days, and 5 days from the same starting point. By overlaying the results of shorter periods on those of longer periods on the plot, approximate results for days 1 to 2, 2 to 3, 3 to 4, and 4 to 5 are obtained.

The model was run at 3-hourly intervals and individual plots were produced. These were then assembled into movies for 1 month intervals, see supporting information for some examples. These movies were invaluable when searching by eye for possible shorter-term correlations.

3. The Link Between Iodine Compounds and Particle Production

Bursts of new particle formation have been observed in the sea ice zone of the Weddell Sea [*Davison et al.,* 1996; *Atkinson et al.,* 2012] over periods of a few hours, with the suggestion that iodine compounds are their source [*Atkinson et al.,* 2012]. Furthermore, analysis of iodine in aerosol samples at Neumayer (Figure S9), although only for 1 year, shows substantial amounts in spring.

Figure 3 shows results from a THAMO model run tuned to give 6 pptv of IO at 5 m above the surface, and Figure 4 from a run tuned to give 20 pptv of IO. The evolution of I_2O_5 is shown in the figures because I_2O_5 is a common precursor in the model to formation of higher iodine oxides that later result in particle production. The figures show that iodine compounds can indeed be the source of particles that can grow to at least 20 nm diameter, provided IO amounts of the order of 20 pptv are produced rather than 6 pptv. Such large values as 20 pptv of IO were indeed observed in late spring 2004 (see Figure S4) and are consistent with SCIAMACHY measurements. Figure 4 predicts dN/dlog(r) well in excess of $10^3 cm^{-3}$ at 10 nm radius (20 nm diameter) with 20 pptv IO. This translates to a number concentration well in excess of $10^2 cm^{-3}$ between 9 and 11 nm radius.
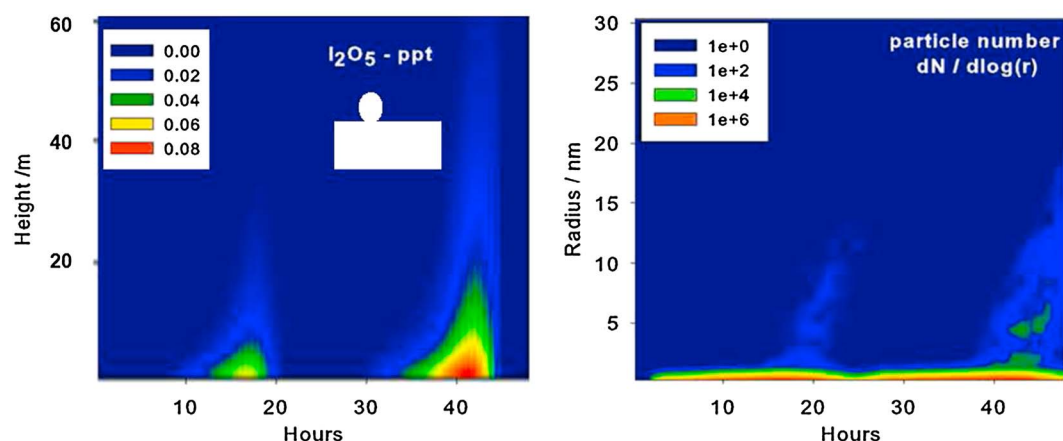
Figure 3. Temporal evolution of the vertical profile of I_2O_5, and of particle size at 5 m altitude, in Antarctic summer from the THAMO model. These results were obtained after tuning surface fluxes of iodine compounds to produce a maximum of 6 pptv of IO at 5 m altitude, this being a value of IO frequently observed at Halley in summer 2004/2005 by long-path DOAS.

Errors in models of formation and growth of particles from iodine oxides are in active research — our model includes the latest known processes, but is not complete. Furthermore, particle number concentration from the model can be very sensitive to the assumed IO concentration and to the assumed surface area of background aerosol due to scavenging. However, although there is a large change in particle number concentration relative to changes in IO concentration at low IO concentrations, the change in particles larger than 20 nm above 15 pptv of IO is relatively small, increasing about fivefold from 15 pptv to 25 pptv [*Mahajan et al.*, 2010, Figure 7]. The change in particle number concentration relative to background aerosol is also nonlinear: a decrease of background surface area from $1e^{-6}$ to $1e^{-7} cm^2 cm^{-3}$ would cause a 100-fold increase in particle number concentration for 15 pptv of IO, but only a tenfold increase for 20 pptv.

Hence, variability in background particles could well confuse any signal in particle density due to iodine compounds. Also, the fact that particle formation from iodine compounds is observed in the laboratory (see section 1) does not mean it would occur in the real world where there may be complicating factors at play. Nevertheless, the above arguments lead us to assume in the analysis below that particles and IO may well be correlated, and so to search for such a correlation.
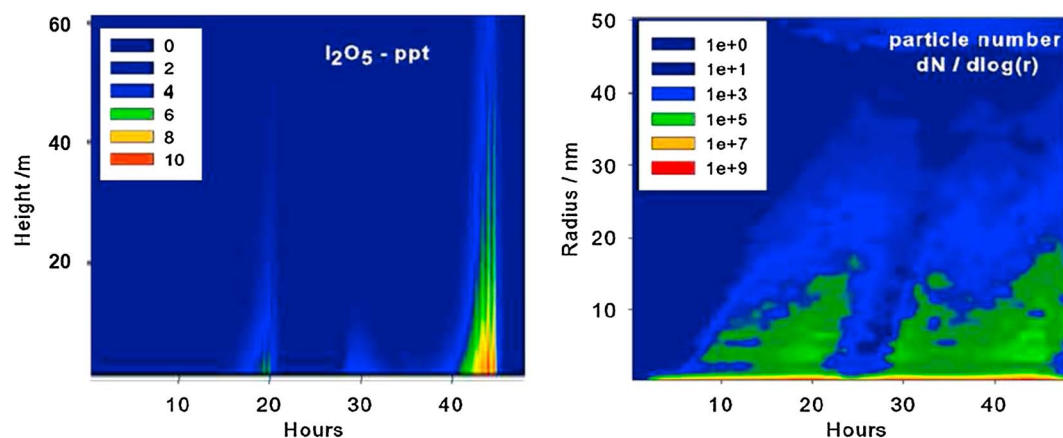

Figure 4. As in Figure 3 but for late spring in Antarctica and after tuning to produce a maximum of 20 pptv of IO at 5 m altitude, this being a value of IO sometimes observed at Halley in late spring 2004. Note the much larger maxima in the color scales than in Figure 3.
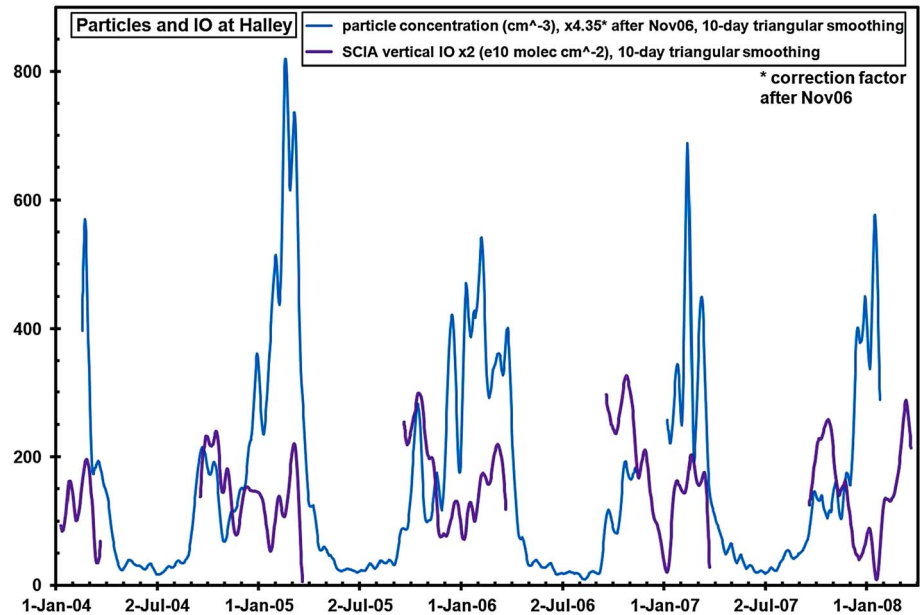
Figure 5. Condensation particle concentrations from measurements at Halley from 2004 to early in 2008, and simultaneous IO vertical amounts from satellite measurements near Halley. The particle concentrations after November 2006 were multiplied by a factor of 4.35, see text and Figure S1 for explanation. Note the secondary maximum in particle concentrations in spring in most years and the spring maximum in IO. Variability can be seen by eye from the changes from week to week in the values.

4. Measurement Results and Analysis

Figure 5 shows a maximum in particle concentration at Halley in austral summer (December/January) or late summer in all years, as at Neumayer in Figure 1. Figure 5 also shows a secondary maximum in particles in austral spring in most years, again as at Neumayer in Figure 1, but the date in spring at Halley varies a little from year to year. In Figure 5, there is good correlation by eye of this secondary maximum in particles with the
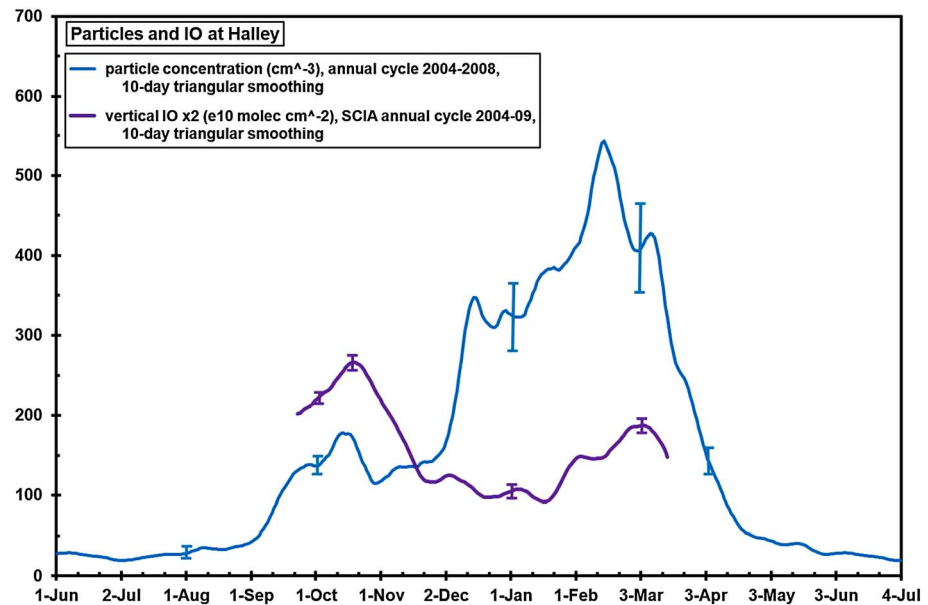

Figure 6. As in Figure 5 but for the annual averages, with one sigma standard errors of selected averages. The coincidence of the spring maximum in IO with the secondary maximum in particles is very pronounced, and the second maximum in IO in the autumn follows the maximum in particles by less than a month.
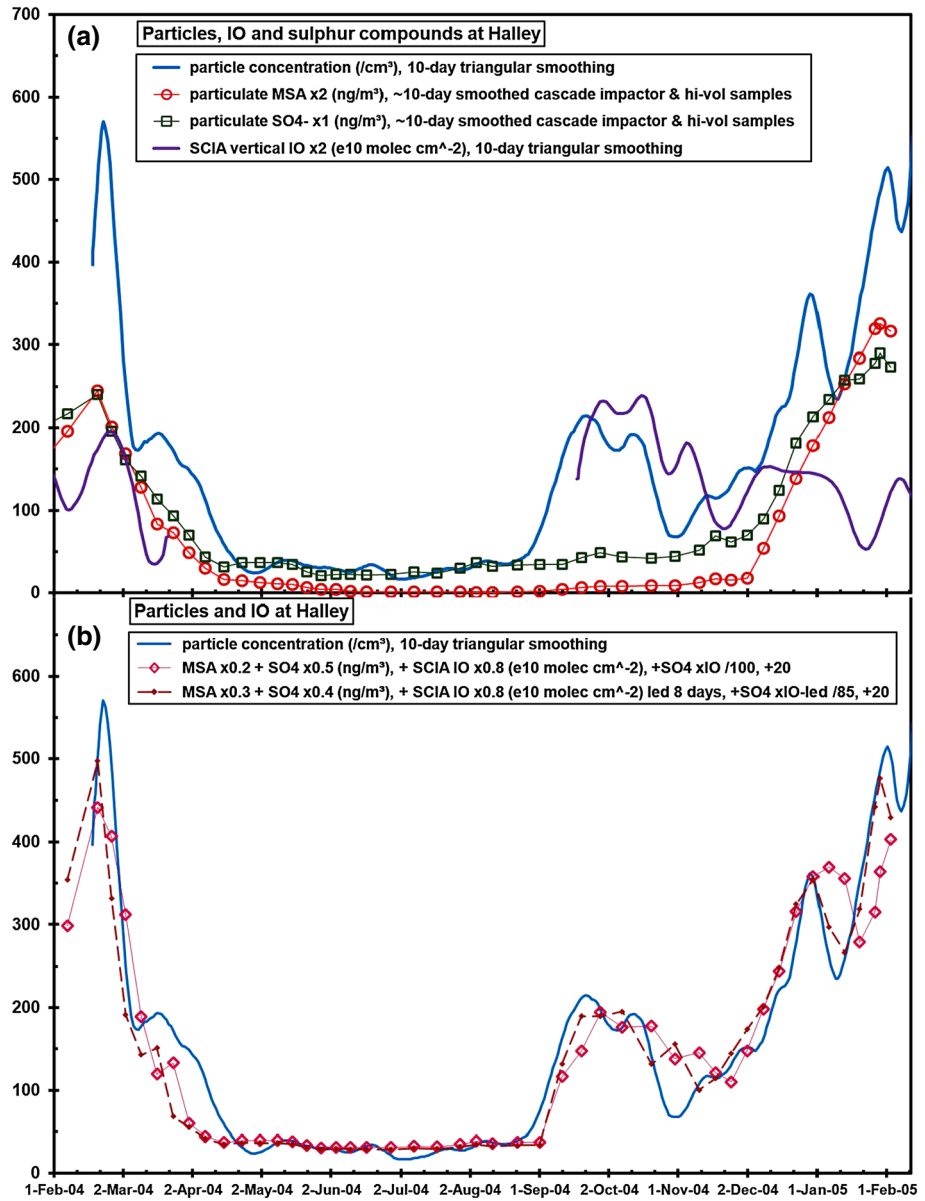
Figure 7. (a) Particles at Halley in 2004 and early 2005, together with sulphur ions in aerosol at Halley and measurements of IO from satellite. (b) Blue line: particles at Halley in 2004 and early 2005; open red diamonds and solid red line: a linear combination of sulphur ions in aerosol at Halley plus IO from satellite plus a term multiplying sulphate by IO plus a constant (see legend for values and text for justification), coefficients were chosen by trial and error; small brown diamonds and dashed line: as open red diamonds, but IO advanced by 8 days and with freshly chosen coefficients.

maximum in IO in the springs of 2004 and 2005; the correlation is still evident in the springs of 2006 and 2007. In 2004 and 2005, there is a strong hint that IO lags the particles by a few days.

This correlation between IO and particles in spring at Halley is striking in the annual average of the data in Figure 6. In this data with more temporal averaging (over 4 years but still 10 day triangular smoothing), there is a strong hint by eye that IO and particles also correlate in austral autumn.

In Figure 7a, the 2004 and early 2005 data are shown together with the cycles of MSA and sulphate ions measured in aerosol sampled simultaneously. It is clear by eye that particles correlate well with sulphur compounds, as expected from the Arctic measurements of *Leaitch et al.* [2013], where new particle production correlated well with MSA. In Figure 7a, particles also correlate well with IO, and it is clear that a linear
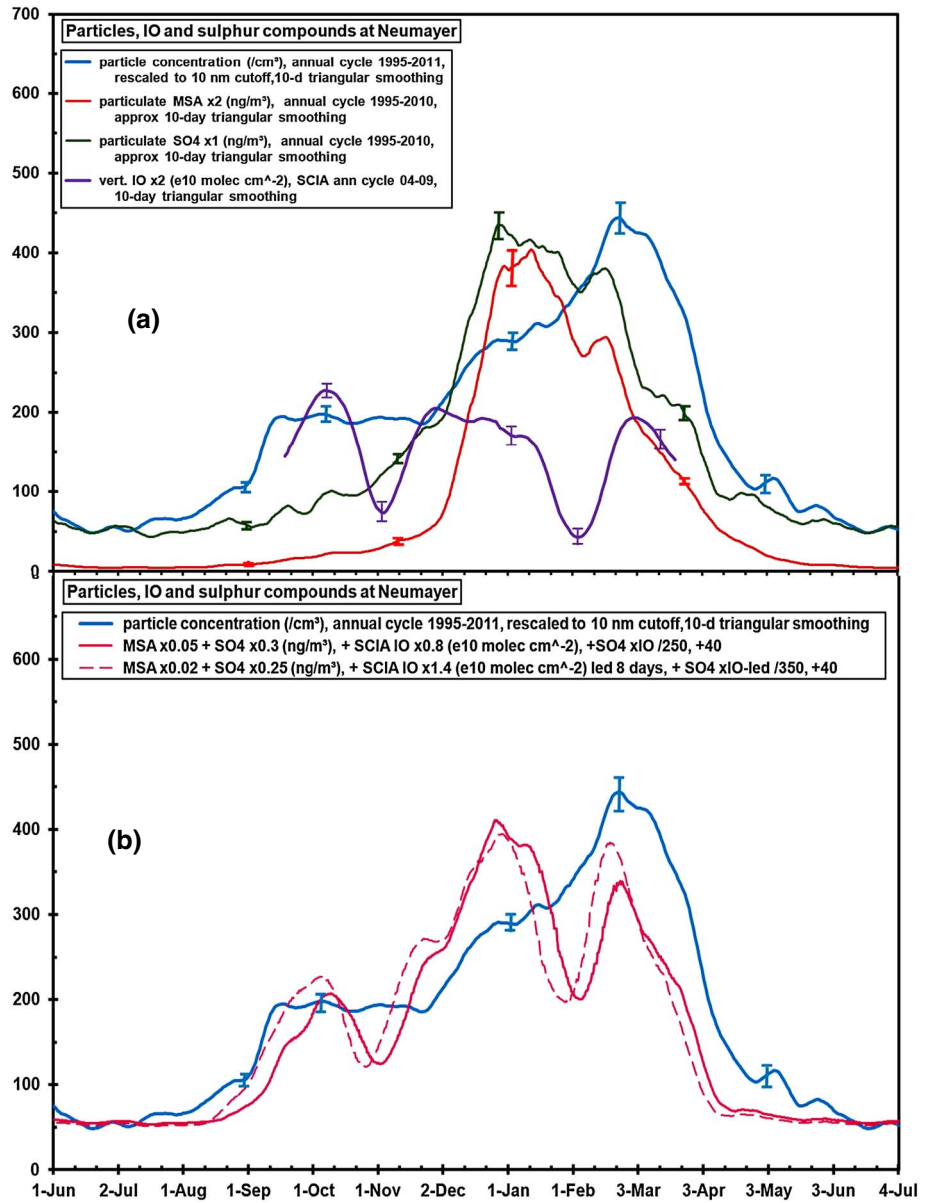
Figure 8. (a) Annual average of particles and sulphur ions in aerosol at Neumayer from 1995 to 2011, together with the annual average of measurements of IO from satellite from 2004 to 2009. (b) Blue line: annual average particles at Neumayer from 1995 to 2011; solid red line: a linear combination of sulphur ions in aerosol at Neumayer plus nearby IO from satellite plus a term multiplying sulphate by IO plus a constant (see legend for values and text for justification), coefficients chosen by trial and error; dashed red line: as solid red line but IO advanced by 8 days and with freshly chosen coefficients. Selected error bars are the one sigma standard errors of the averages.

combination of IO and sulphur compounds could produce a good match with aerosol. There is a strong suggestion that the IO data lags the particle data by about 8 days.

Figure 7b shows our attempt to make such a linear combination by eye, which produces a useful result. Because we expect iodine particles to be more viable if they are further grown by sulphate, we have included a cross-term multiplying IO by sulphate; because we might expect additional particles from evaporated sea spray throughout the year (not included in sulphate or MSA terms), we have also included a small constant term. The correlation is good if the IO data are included without a lag, but Figure 7b shows the result further improved if the IO data are moved forward in time by 8 days before including it in the linear combination, as expected from the lag in Figure 7a. Note that the results in Figure 7 do not include
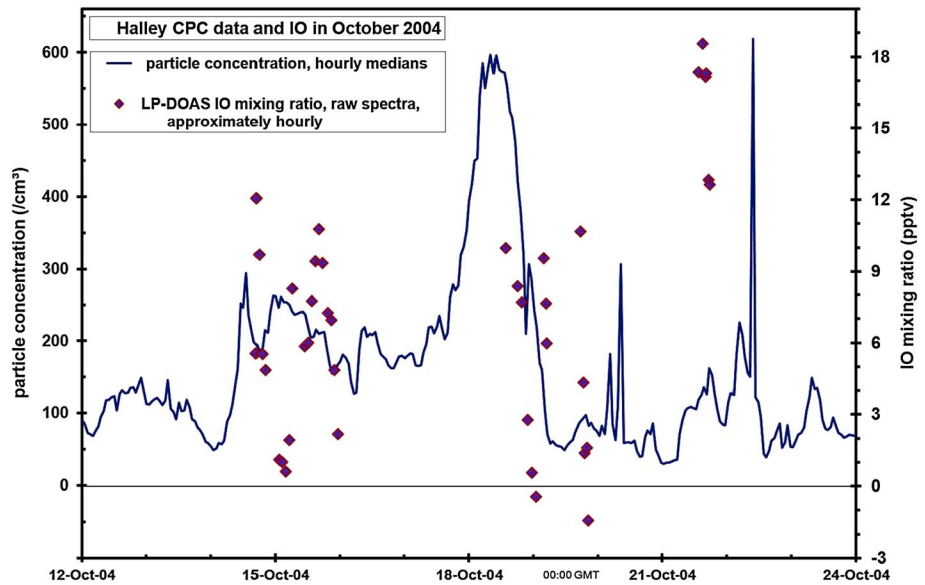
Figure 9. Hourly measurements of particles and IO at Halley in October 2004. The IO measurements were not continuous because on some days the distant reflector could not be properly seen, and because the spectrometer was routinely switched from the visible wavelengths of the IO observations to the UV wavelengths of BrO observations.

the second and third periods of operation of the Halley CPC (see section 2.1.1), for which corrections had to be made.

The optimum iodine-particle lag at Halley varies throughout the year, but it is not clear that it is a consistent seasonal variation (e.g., longer in spring than autumn). To investigate, this would demand sophisticated lag regressions and more years of sulphate and MSA data.

At Neumayer, there are many more years of measurements of particles and sulphur compounds (e.g., Figure 1), so we can produce a smoother annual average. Figure 8a shows the result, although there are many fewer years
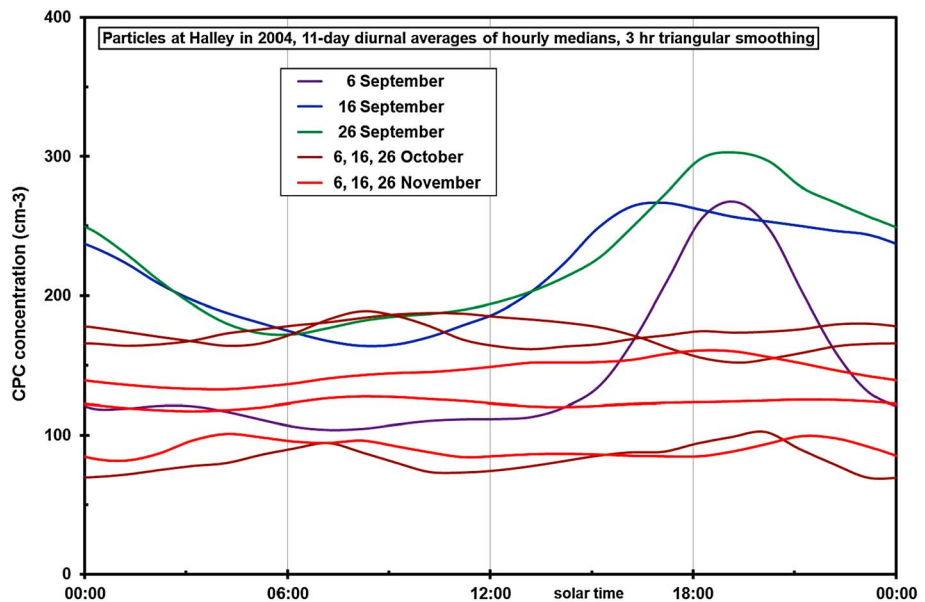

Figure 10. Diurnal changes in particles at Halley in spring and early summer 2004. These are hourly medians, averaged by hour over 11 days centered at each date listed, and smoothed with a triangular function of full width at half maximum 3 days, after wrapping around at each end of the diurnal period.
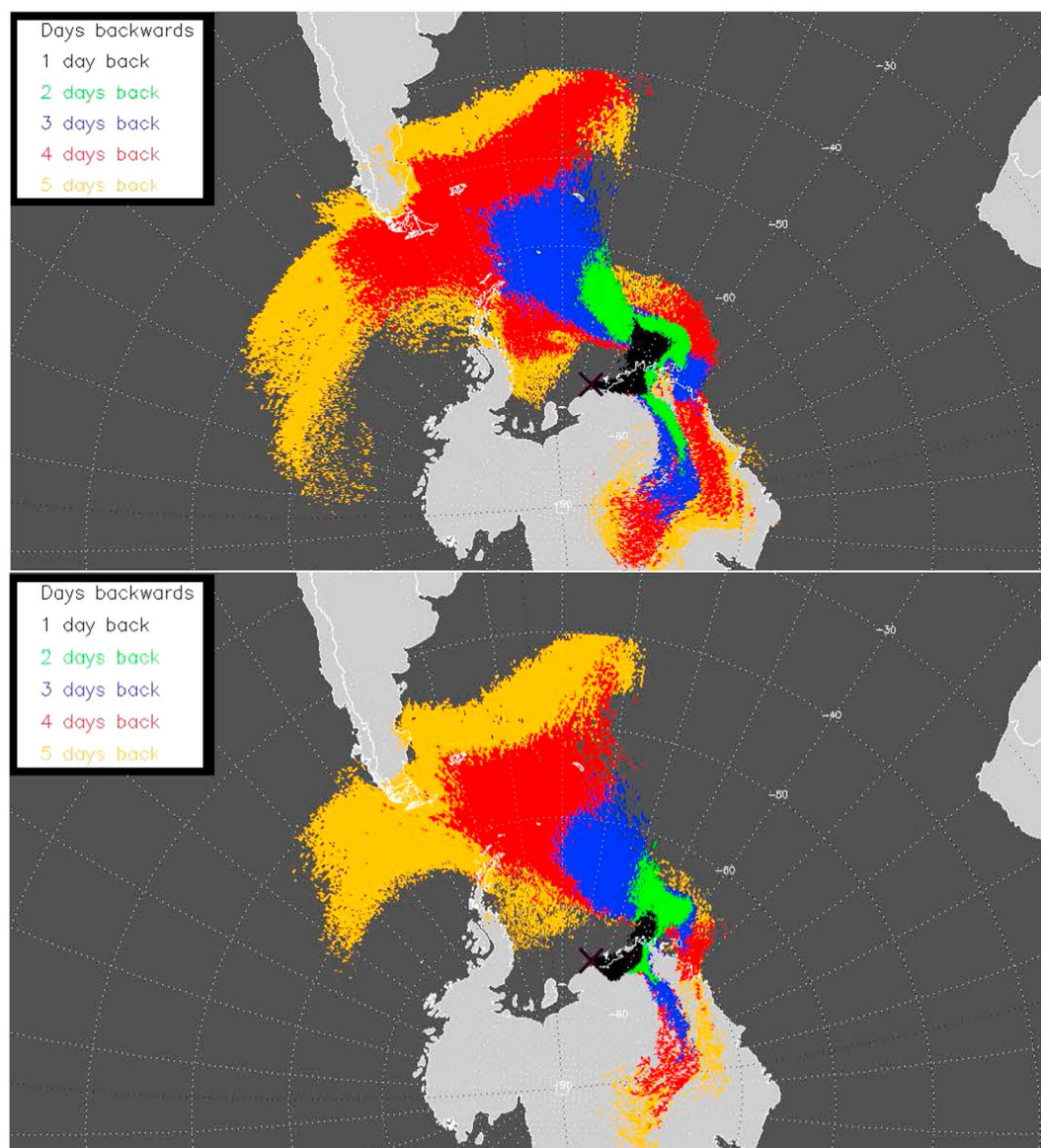
Figure 11. Back trajectories from Halley from (top) 17 October 2004 at 18:00 to (bottom) 18 October 2004 at 12:00.

of IO data than particle data. Again, a combination of sulphur compounds and IO gives a useful fit, again more so if the IO data are led by 8 days (Figure 8b).

The fits in Figure 8 are less good than those for Halley data in Figure 7 and are poor without the constant and IO times sulphate terms (not shown), unlike for Halley data (also not shown). This is probably because the IO at Neumayer does not decrease markedly in midsummer, unlike at Halley—compare the purple lines in Figures 8a and 6.

Examination of other years of particle and IO measurements from Halley between 2005 and 2008 (not shown) shows that the apparent lag between IO and particles varies between 0 and about 15 days; examination of individual years from Neumayer produces a similar result, hence the improved fit with a lag of 8 days. Although the centers of the simultaneous IO satellite measurements are displaced from the particle measurement sites, to the south-east or south by 200 km, this is not enough to cause such a lag: typical wind speeds at Halley are 2 to 20 m/s (7 to 70 km/h), far too large to give an 8 day lag. Winds would have to be consistently 1 km/h (0.3 m/s) for this displacement to cause an 8 day lag. In section 6, we speculate about a possible explanation for such a lag.

5. Lack of Short-Term Correlation Between IO and Particles

The strong evidence for iodine compounds being responsible for new particle production in the sea ice zone might lead us to expect particles and iodine monoxide to be correlated on shorter-time scales.

However, there is no evidence in the Halley data for correlation on time scales shorter than 2 days or less. Figure 9 shows measurements of IO at approximately 1 h intervals by the long-path DOAS in October 2004, together with simultaneous measurements of particles at Halley. The enhancement in IO on 21 October is not correlated with any nearby enhancement in particles. The enhancement in particles on 18 October is not correlated with any enhancement in IO over that observed 3 days earlier. Another example of the lack of correlation is given in the supporting information Figure S7.

There is also little evidence for short-term correlation between IO and particles from the diurnal change in particles. In September 2004, when SCIAMACHY shows there to be significant IO, particles are indeed a maximum in the late afternoon (Figure 10), as suggested by model results, but in October and early November 2004, when the long-path DOAS also shows there to be significant IO, diurnal change in particles in Figure 10 becomes negligible.

There is little evidence of correlation of particles with source locations in the shorter term during October 2004, from the trajectories calculated backward from Halley. Figure 11 shows only modest differences in back trajectories between late afternoon on 17 October and noon on 18 October, when Figure 9 shows particle concentration doubled. A visual analysis of the trajectory movies for October and December 2004 in the supporting information shows that at other times trajectories vary to a much larger degree. Again, there is no obvious correlation with Figure 9 or with Figure S7. In section 6, we speculate about why this might be.

6. Conclusions and Further Work

We conclude that iodine compounds may contribute to the secondary production of significant numbers of aerosol particles measured by Condensation Particle Counters on the Weddell Sea coast during spring, because of the clear correlation we observe between IO and particle density. Of course, given our limited data set, it is also possible that other halogenated and organic compounds may be responsible for the increase in particle density we observe in spring.

The correlation we observe between IO and particle density seems to be improved if the IO is lagged by about 8 days, which leads us to suggest that many of the iodine compounds and associated particle production occur some distance offshore. We speculate that the time taken for reactive iodine compounds (I_y, of which IO is the dominant daytime constituent) to travel from their offshore source may be longer than the time taken for particles, because the I_y is recycled via the snow or ice surface, and the recycling is dominated by sunlight photolysis which is only available for half the time in the spring. Such a process would account for a lag between periods of enhanced particle number concentration and enhanced IO, and it would account for the variability of the lag as wind speeds, distances to the production area and availability of daylight vary.

The discrepancy between our model output, which predicts about 10^4 particles/cm^3 during enhanced IO, while only about some hundreds were observed at the coast, suggests that for particles at the coast the nucleation mode may have already grown into larger modes. This possibility that particles were somewhat aged supports the hypothesis of their initial production some distance offshore.

The approach in this paper neglects the importance of particle size distribution because such measurements were not available at Halley, apart from limited chemical speciation of filtered aerosol, in the period we discuss. As shown by *Weller et al.* [2011], high particle number concentrations in combination with only moderate sulphur concentrations observed at Neumayer in March may have been caused by nucleation and/or Aitken mode particles, which do not contribute much to aerosol mass. This fact may blur a more clear correlation between the total particle concentrations shown above and chemical species.

Future work on the sources of particles in the sea ice zone should include the following:

1. Analysis of further years of filtered aerosol at Halley, where samples from 2005 to 2008 have been gathered but not yet analyzed for ionic content.
2. Modeling work that can examine the possible production of particles some distance offshore, and their effect on measurements at coastal sites.

This second item would necessitate runs with a regional or global model that included schemes for iodine chemistry, aerosol production, and interactions with sea ice and snow — a one-dimensional model such as THAMO cannot hope to capture these processes over a large area and distance.

References

Atkinson, H. M., R.-J. Huang, R. Chance, H. K. Roscoe, C. Hughes, B. Davison, A. Schönhardt, A. S. Mahajan, A. Saiz-Lopez, and P. S. Liss (2012), Iodine emissions from the sea ice of the Weddell Sea, *Atmos. Chem. Phys.*, *12*, 11,229–11,244, doi:10.5194/acp-12-11229-2012.

Bloss, C., et al. (2005), Development of a detailed chemical mechanism (MCMv3.1) for the atmospheric oxidation of aromatic hydrocarbons, *Atmos. Chem. Phys.*, *5*, 641–664.

Charlson, R. J., J. E. Lovelock, M. O. Andreae, and S. G. Warren (1987), Oceanic phytoplankton, atmospheric sulphur, cloud albedo and climate, *Nature*, *326*, 655–661.

Cosme, E., F. Hourdin, C. Genthon, and P. Martinerie (2005), Origin of dimethylsulfide, non-sea-salt sulfate, and methanesulfonic acid in eastern Antarctica, *J. Geophys. Res.*, *110*, D03302, doi:10.1029/2004JD004881.

Davison, B., C. N. Hewitt, C. D. O'Dowd, J. A. Lowe, M. H. Smith, M. Schwikowski, U. Baltensperger, and R. M. Harrison (1996), Dimethyl sulfide, methane sulfonic acid and physicochemical aerosol properties in Atlantic air from the United Kingdom to Halley Bay, *J. Geophys. Res.*, *101*, 22,855–22,867, doi:10.1029/96JD01166.

Dix, B., S. Baidar, J. F. Bresch, S. R. Hall, K. S. Schmidt, S. Wang, and R. Volkamer (2013), Detection of iodine monoxide in the tropical free troposphere, *Proc. Natl. Acad. Sci. U.S.A.*, *110*, 2035–2040, doi:10.1073/pnas.1212386110.

Jones, A., D. Thomson, M. Hort, and B. Devenish (2007), The UK Met Office's next generation atmospheric dispersion model, NAME III, in *Air Pollution Modeling and Its Application XVII*, vol. 17, pp. 580–589, Springer, New York.

Jones, A. E., et al. (2008), Chemistry of the Antarctic boundary layer and the interface with snow: An overview of the CHABLIS campaign, *Atmos. Chem. Phys.*, *8*, 3789–3803.

Leaitch, W. R., et al. (2013), Dimethyl sulfide control of the clean summertime Arctic aerosol and cloud, *Elementa*, *1*, 000017, doi:10.12952/journal.elementa.000017.

Mahajan, A. S., J. M. C. Plane, H. Oetjen, L. Mendes, R. W. Saunders, A. Saiz-Lopez, C. E. Jones, L. J. Carpenter, and G. B. McFiggans (2010), Measurement and modelling of tropospheric reactive halogen species over the tropical Atlantic Ocean, *Atmos. Chem. Phys.*, *10*, 4611–4624, doi:10.5194/acp-10-4611-2010.

Obbard, R. W., H. K. Roscoe, E. W. Wolff, and H. M. Atkinson (2009), Frost flower surface area and chemistry as a function of salinity and temperature, *J. Geophys. Res.*, *114*, D20305, doi:10.1029/2009JD012481.

O'Dowd, C. D., J. L. Jimenez, R. Bahreini, R. C. Flagan, J. H. Seinfeld, K. Hameri, L. Pirjolak, M. Kulmala, S. G. Jennings, and T. Hoffmann (2002), Marine aerosol formation from biogenic iodine emissions, *Nature*, *417*, 632–636.

Rankin, A. M., and E. W. Wolff (2003), A year-long record of size-segregated aerosol composition at Halley, Antarctica, *J. Geophys. Res.*, *108*(D24), 4775, doi:10.1029/2003JD003993.

Saiz-Lopez, A., A. S. Mahajan, R. A. Salmon, S. J.-B. Bauguitte, A. E. Jones, H. K. Roscoe, and J. M. C. Plane (2007), Boundary layer halogens in coastal Antarctica, *Science*, *317*, 348–351.

Saiz-Lopez, A., et al. (2008), On the vertical distribution of boundary layer halogens over coastal Antarctica: Implications for O_3, HO_x, NO_x and the Hg lifetime, *Atmos. Chem. Phys.*, *8*, 887–900.

Saiz-Lopez, A., J. M. C. Plane, A. R. Baker, L. J. Carpenter, R. von Glasow, J. C. G. Martin, G. McFiggans, and R. W. Saunders (2012), Atmospheric chemistry of iodine, *Chem. Rev.*, *112*, 1773–1804, doi:10.1021/cr200029u.

Sander, S. P., et al. (2006), Chemical Kinetics and Photochemical Data for use in Atmospheric Studies, Evaluation Number 15, JPL Publication 06-2, Jet Propul. Lab., Pasadena, Calif.

Saunders, R. W., R. Kumar, J. C. G. M. Martin, A. S. Mahajan, B. J. Murray, and J. M. C. Plane (2010), Studies of the formation and growth of aerosol from molecular iodine precursor, *Z. Phys. Chem.*, *224*, 1095–1117, doi:10.1524/zpch.2010.6143.

Saunders, S. M., M. E. Jenkin, R. G. Derwent, and M. J. Pilling (2003), Protocol for the development of the Master Chemical Mechanism, MCM v3 (part A): Tropospheric degradation of non-aromatic volatile organic compounds, *Atmos. Chem. Phys.*, *3*, 161–180.

Schönhardt, A., A. Richter, F. Wittrock, H. Kirk, H. Oetjen, H. K. Roscoe, and J. P. Burrows (2008), Observations of iodine monoxide (IO) columns from satellite, *Atmos. Chem. Phys.*, *8*, 637–653.

Weller, R., A. Minikin, D. Wagenbach, and V. Dreiling (2011), Characterization of the inter-annual, seasonal, and diurnal variations of condensation particle concentrations at Neumayer, Antarctica, *Atmos. Chem. Phys.*, *11*, 13,243–13,257, doi:10.5194/acp-11-13243-2011.